

## DETC'01/VIB-??????

### A COMPONENT MODE SYNTHESIS LOOK AT PLANAR BEAM ELEMENTS<sup>1</sup>

**J. P. Meijaard and A. L. Schwab**  
Laboratory for Engineering Mechanics  
Delft University of Technology  
Mekelweg 2, NL-2628 CD Delft  
The Netherlands  
Email: j.p.meijaard@wbmt.tudelft.nl

#### KEYWORDS

Flexible multibody dynamics; finite element method; planar beam elements; geometric stiffness.

#### ABSTRACT

This paper deals with the improvement in efficiency of simulations in flexible multibody system dynamics. On the basis of concepts from component mode synthesis techniques some improved elements for planar beams which are hinged at one or both ends are developed. These elements show a considerable increase in accuracy, or alternatively allow a reduction of the number of elements, with respect to a standard element with cubic polynomial interpolation. The use of the elements is demonstrated in two examples: a planar slider-crank mechanism with a flexible connecting rod and a cantilevered beam in a spin-up motion.

#### INTRODUCTION

In order to describe complex mechanical systems in sufficient detail, finite element models with many degrees of freedom are employed. Often many elements are needed to describe details of the shape and the stiffness and stress distribution. Owing to the many re-evaluations needed in a dynamic analysis, it is important to reduce the number of degrees of freedom as much as possible, while the behaviour of the system is still described with sufficient accuracy. Moreover, by the reduction the stiffness

of the system of the differential equations decreases, which allows larger step sizes in explicit numerical integration methods, and the overall speed-up of the computational process is considerable.

A common approach to the reduction of a system is to use a hierarchical description in which the system is divided into components, or substructures, or superelements, which themselves are modelled by subcomponents or elements. The motion of each component is approximated by a linear combination of some modes that are far less numerous than the degrees of freedom in the detailed model. The reduced equations of motion for each subsystem are obtained from the principle of virtual work, while the equations of motion of the complete system are formed by combining these component equations and introducing the connections between the components. Hunn (Hunn, 1953; Hunn, 1955) first used this technique for linear vibration problems. Hurty (Hurty, 1960) introduced the designation *component mode synthesis* for it. Several variants were developed which differ in the way the modes are selected. A class of modes are vibration modes of the substructure with different kinds of boundary conditions, for instance clamped interfaces as used by Hurty (Hurty, 1965) and Craig and Bampton (Craig and Bampton, 1968). These modes are supplemented by some static modes, as used in static condensation (Guyan, 1965; Irons, 1965). Another choice of modes which depend on the way in which the substructure is loaded was proposed by Wilson, Yuan and Dickens (Wilson *et al.*, 1982) and generalized by Léger (Léger, 1988). The application of component modes to describe

<sup>1</sup>Dedicated to the memory of Dr R. Schwertassek.

small deformations of bodies which undergo large rotations was shown in (Shabana and Wehage, 1983); load-dependent modes were used in (Yeh and Dopker, 1990). Further references to the extensive literature can be found in several review articles; Noor (Noor, 1994) discusses general reduction methods, while reviews on component mode synthesis methods are given in (Craig, 1981; Greif, 1986; Craig, 1995; Seshu, 1996).

In this paper some methods for building superelements for components are applied to beams in planar motion. It is argued and shown in an example that the use of the proper load-dependent modes for the deformations leads to the most satisfactory results. Besides, the inclusion of non-linear terms in the combination of modes which capture geometric non-linearities is shown to be possible.

In the next section, the finite element approach to modelling multibody systems is reviewed and several versions of a planar beam element are derived. Then the elements are applied in two examples: a slider-crank mechanism with a flexible connecting rod and a cantilevered beam in a spin-up motion. The paper ends with some conclusions.

## PLANAR BEAM ELEMENTS

### Formulation of the Equations of Motion

The finite element method as presented in (Jonker, 1989; Jonker and Meijaard, 1990; Meijaard, 1991) is used for building models for flexible multibody systems. A model for a system is built up from elements which are connected at nodes. A typical element  $e$  has a number of nodes with nodal coordinates  $\mathbf{x}^e$ , which may include Cartesian position coordinates and coordinates that parametrize rotations. Generalized deformations, or strains,  $\varepsilon^e$ , are related to the nodal coordinates by deformation functions as  $\varepsilon^e = \mathbf{D}^e(\mathbf{x}^e)$ , which are invariant under arbitrary rigid-body displacements. Each element gives a contribution to the virtual work of the system, where inertia terms are included according to D'Alembert's principle and ideal constraint forces which eventually drop out of the equations need not be included, of the form

$$\delta \mathbf{x}^e \cdot [\mathbf{f}^e - \mathbf{M}^e \ddot{\mathbf{x}}^e] - \delta \varepsilon^e \cdot \boldsymbol{\sigma}^e. \quad (1)$$

Here,  $\mathbf{f}^e = \mathbf{f}^{ea} - \mathbf{h}^e$  is the element force vector, which contains the element applied forces  $\mathbf{f}^{ea}$  and inertia terms  $\mathbf{h}^e$  that are related to the element mass matrix  $\mathbf{M}^e$  as

$$h_i^e = \sum_{j,k} \left( \frac{\partial M_{ij}^e}{\partial x_k^e} - \frac{1}{2} \frac{\partial M_{jk}^e}{\partial x_i^e} \right) \dot{x}_j^e \dot{x}_k^e. \quad (2)$$

The generalized element stresses,  $\boldsymbol{\sigma}^e$ , are energetically dual to the generalized strains and are related to the strains by constitu-

tive equations. The prefix  $\delta$  denotes a virtual quantity, where the virtual strains are related to the virtual displacements by  $\delta \varepsilon_i^e = \sum_j (\partial D_i^e / \partial x_j) \delta x_j^e$ . The contributions of the nodes to the virtual work of the system have a similar form with the main difference that nodes do not have generalized deformations.

In order to obtain the equations of motion for the system, global vectors of nodal coordinates  $\mathbf{x}$ , deformation functions  $\mathbf{D}(\mathbf{x})$ , strains  $\varepsilon = \mathbf{D}(\mathbf{x})$ , forces  $\mathbf{f}$ , stresses  $\boldsymbol{\sigma}$  and a global mass matrix  $\mathbf{M}$  are introduced and all contributions to the virtual work are collected as

$$\delta \mathbf{x} \cdot [\mathbf{f}(\dot{\mathbf{x}}, \mathbf{x}, t) - \mathbf{M}(\mathbf{x}) \ddot{\mathbf{x}}] - \delta \varepsilon \cdot \boldsymbol{\sigma} = 0. \quad (3)$$

The nodal coordinates  $\mathbf{x}$  are related to the vector of independent coordinates  $\mathbf{q}$  by transfer functions  $\mathbf{F}^x$  as  $\mathbf{x} = \mathbf{F}^x(\mathbf{q}, t)$ . Similarly the element deformations are related to the independent coordinates by transfer functions as  $\varepsilon = \mathbf{F}^\varepsilon(\mathbf{q}, t) = \mathbf{D}(\mathbf{F}^x(\mathbf{q}, t))$ . These transfer functions have to be consistent with the constraints of the system and are not generally known in an explicit form, but have to be determined by a numerical iterative process. For holonomic systems, one can obtain expressions for the velocities, accelerations and virtual displacements by differentiation of the transfer functions. By substituting these in Eq. (3) and making use of the fact that the variations  $\delta \mathbf{q}$  are independent, we obtain the equations of motion for the system:

$$\bar{\mathbf{M}}(\mathbf{q}, t) \ddot{\mathbf{q}} = \bar{\mathbf{f}}(\dot{\mathbf{q}}, \mathbf{q}, t). \quad (4)$$

Here,  $\bar{\mathbf{M}}$  is the system mass matrix and  $\bar{\mathbf{f}}$  is the system force vector.

### Planar Beam Elements: General Considerations

In a finite element formulation, a section of a beam that moves in a single plane is modelled by a planar beam element. It is assumed that this beam section has a uniform cross-section with uniform linearly elastic isotropic material properties. The mass density is  $\rho$ , Young's modulus is  $E$ , the cross-sectional area is  $A$  and the central area moment of inertia is  $I$ . The undeformed length of the beam section is  $l_0$ . Use is made of the elastic line concept, where all properties are considered to be concentrated on the elastic line that runs along the centroid of the cross-section, and the classical Euler-Bernoulli beam theory is used.

All beam elements that are considered in this paper have two nodes, which represent the end points of the beam section that is modelled by the element. The nodes have two Cartesian coordinates,  $x$  and  $y$ , and an orientation angle,  $\phi$ , as their coordinates. If the element  $e$  is connected to the nodes  $p$  and  $q$ , the element coordinates are (Fig. 1)

$$\mathbf{x}^{eT} = (x^p, y^p, \phi^p, x^q, y^q, \phi^q). \quad (5)$$

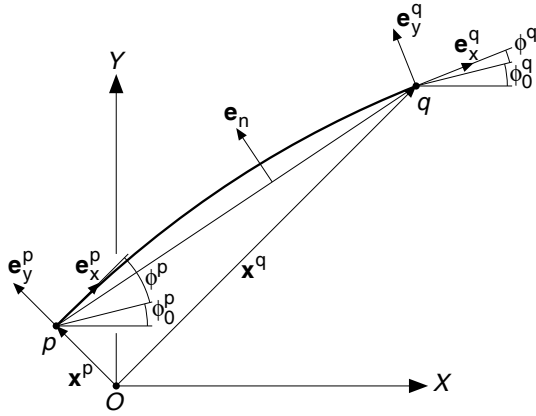


Figure 1. Planar beam element.

For later reference, we first introduce the nodal position vector  $\mathbf{x}^{pT} = (x^p, y^p)$  and a pair of unit vectors at the node  $p$  as

$$\mathbf{e}_x^p = \begin{pmatrix} \cos(\phi^p + \phi_0^p) \\ \sin(\phi^p + \phi_0^p) \end{pmatrix}, \quad \mathbf{e}_y^p = \begin{pmatrix} -\sin(\phi^p + \phi_0^p) \\ \cos(\phi^p + \phi_0^p) \end{pmatrix}, \quad (6)$$

where  $\phi_0^p$  defines the angle with which the beam is connected to the node; similar quantities are defined for the node  $q$ . The vector connecting the node  $p$  to the node  $q$  is denoted by  $\Delta \mathbf{x}^e$ ,  $\Delta \mathbf{x}^e = \mathbf{x}^q - \mathbf{x}^p$ , and its length by  $l$ ,  $l^2 = \Delta \mathbf{x}^e \cdot \Delta \mathbf{x}^e$ .

The generalized deformations of the element are the elongation of the axis of the beam and two bending modes. The elongation of the beam,

$$\varepsilon_1^e = \frac{l^2 - l_0^2}{2l_0} + \varepsilon^{nl}(l_0, \varepsilon_2^e, \varepsilon_3^e), \quad (7)$$

is given by the Lagrangian strain measure for the change of the distance between the two nodal points, augmented by a non-linear contribution of the bending to the elongation of the axis,  $\varepsilon^{nl}$ , which is different for different variants and depends on the undeformed length of the beam and the two bending deformations  $\varepsilon_2^e$  and  $\varepsilon_3^e$ . These bending deformations are defined by

$$\varepsilon_2^e = -\mathbf{e}_y^p \cdot \Delta \mathbf{x}^e, \quad \varepsilon_3^e = \mathbf{e}_y^q \cdot \Delta \mathbf{x}^e. \quad (8)$$

The element properties are arrived at by assuming an interpolation for the position of the elastic line of the deformed beam. Conceptually, one can split the beam in two elements, a beam element to which mass is attached, but which has no stiffness and can deform freely, and a massless beam element with stiffness.

These two elements are forced to move together, because they share their nodal points. This splitting of the beam allows us to assume independent interpolations for the description of the inertia distribution and accelerations at the one hand and for the deformations at the other hand; these two, however, have to differ little for small deformations of the beam and are preferably the same in the linearized case. The gained freedom allows us to simplify expressions as much as possible.

In the interpolation for the position, the material coordinate  $s$ , measured along the undeformed length of the beam from the node  $p$  with  $0 \leq s \leq l_0$ , and the dimensionless material coordinate  $\xi = s/l_0$  with  $0 \leq \xi \leq 1$  are introduced. For the mass description, the position  $\mathbf{r}$  of a point along the elastic line with coordinate  $\xi$  is found from an interpolation of the form

$$\mathbf{r}(\xi) = h_1(\xi)\mathbf{x}^p + h_2(\xi)l_0\mathbf{e}_x^p + h_3(\xi)\mathbf{x}^q + h_4(\xi)l_0\mathbf{e}_x^q. \quad (9)$$

For rigid-body motions,  $\mathbf{r}(\xi) = (1 - \xi)\mathbf{x}^p + \xi\mathbf{x}^q$  and  $l_0\mathbf{e}_x^p = l_0\mathbf{e}_x^q = \mathbf{x}^q - \mathbf{x}^p$ , so in order to be able to describe rigid-body motions exactly, the interpolation functions have to satisfy the relations

$$h_1 - h_2 - h_4 = 1 - \xi, \quad h_2 + h_3 + h_4 = \xi. \quad (10)$$

By differentiation one finds expressions for the accelerations and the virtual displacements as

$$\ddot{\mathbf{r}}(\xi) = h_1(\xi)\ddot{\mathbf{x}}^p + h_2(\xi)l_0(\mathbf{e}_y^p\ddot{\phi}^p - \mathbf{e}_x^p(\dot{\phi}^p)^2) + h_3(\xi)\ddot{\mathbf{x}}^q + h_4(\xi)l_0(\mathbf{e}_y^q\ddot{\phi}^q - \mathbf{e}_x^q(\dot{\phi}^q)^2), \quad (11)$$

$$\delta \mathbf{r}(\xi) = h_1(\xi)\delta \mathbf{x}^p + h_2(\xi)l_0\mathbf{e}_y^p\delta\phi^p + h_3(\xi)\delta \mathbf{x}^q + h_4(\xi)l_0\mathbf{e}_y^q\delta\phi^q. \quad (12)$$

Evaluating the inertia term in the virtual work equation,  $-\rho A l_0 \int_0^1 \delta \mathbf{r}(\xi) \cdot \ddot{\mathbf{r}}(\xi) d\xi$ , results in an element mass matrix

$$\mathbf{M}^e = \rho A l_0 \begin{bmatrix} \mu_{11}\mathbf{I}_2 & \mu_{12}l_0\mathbf{e}_y^p & \mu_{13}\mathbf{I}_2 & \mu_{14}l_0\mathbf{e}_y^q \\ \mu_{21}l_0\mathbf{e}_y^{pT} & \mu_{22}l_0^2 & \mu_{23}l_0\mathbf{e}_y^{pT} & \mu_{24}l_0^2\mathbf{e}_y^p \cdot \mathbf{e}_y^q \\ \mu_{31}\mathbf{I}_2 & \mu_{32}l_0\mathbf{e}_y^p & \mu_{33}\mathbf{I}_2 & \mu_{34}l_0\mathbf{e}_y^q \\ \mu_{41}l_0\mathbf{e}_y^{qT} & \mu_{42}l_0^2\mathbf{e}_y^q \cdot \mathbf{e}_y^p & \mu_{43}l_0\mathbf{e}_y^{qT} & \mu_{44}l_0^2 \end{bmatrix}, \quad (13)$$

where  $\mathbf{I}_2$  is the identity matrix of order two, and the terms that are quadratic in the velocities,

$$\mathbf{h}^e = \rho A l_0 \begin{bmatrix} -\mu_{12}l_0\mathbf{e}_x^p(\dot{\phi}^p)^2 - \mu_{14}l_0\mathbf{e}_x^q(\dot{\phi}^q)^2 \\ -\mu_{24}l_0^2\mathbf{e}_y^p \cdot \mathbf{e}_y^q(\dot{\phi}^q)^2 \\ -\mu_{32}l_0\mathbf{e}_x^p(\dot{\phi}^p)^2 - \mu_{34}l_0\mathbf{e}_x^q(\dot{\phi}^q)^2 \\ -\mu_{42}l_0^2\mathbf{e}_y^q \cdot \mathbf{e}_y^p(\dot{\phi}^p)^2 \end{bmatrix}, \quad (14)$$

where the numerical coefficients  $\mu_{ij}$  are given by the integrals

$$\mu_{ij} = \int_0^1 h_i(\xi)h_j(\xi)d\xi. \quad (15)$$

For the description of the stiffness, an interpolation is used that differs slightly from the interpolation for the mass description as in Eq. (9). As an auxiliary quantity, a unit vector  $\mathbf{e}_n$  perpendicular to the straight line connecting the two nodes,  $\mathbf{e}_n^T = (-y^q + y^p, x^q - x^p)/l$ , is introduced, see Fig. 1. The interpolation of the position along the beam is chosen as

$$\mathbf{r}(\xi) = (1 - \xi)\mathbf{x}^p + \xi\mathbf{x}^q + (h_2(\xi)\varepsilon_2^e - h_4(\xi)\varepsilon_3^e)\mathbf{e}_n. \quad (16)$$

As a measure for the curvature of the beam we take

$$\kappa = \mathbf{e}_n \cdot \frac{\partial^2 \mathbf{r}}{\partial s^2} = \frac{1}{l_0^2} (h_2''\varepsilon_2^e - h_4''\varepsilon_3^e), \quad (17)$$

where primes denote derivatives with respect to  $\xi$ . The bending moment is proportional to this curvature with proportionality factor  $EI$ .

As a measure for the axial strain we take

$$\gamma = \frac{1}{2} \left[ \frac{\partial \mathbf{r}}{\partial s} \cdot \frac{\partial \mathbf{r}}{\partial s} - 1 \right] = \frac{1}{2l_0^2} [l^2 - l_0^2 + (h_2'\varepsilon_2^e - h_4'\varepsilon_3^e)^2]. \quad (18)$$

In order to comply with the definition of the generalized strain as given in Eq. (7), the axial strain is integrated over the material length of the element, which yields

$$\varepsilon^{nl} = \frac{1}{2l_0} [\beta_{22}(\varepsilon_2^e)^2 - 2\beta_{24}\varepsilon_2^e\varepsilon_3^e + \beta_{44}(\varepsilon_3^e)^2], \quad (19)$$

where the numerical coefficients  $\beta_{ij}$  are given by the integrals

$$\beta_{ij} = \int_0^1 h_i'(\xi)h_j'(\xi)d\xi. \quad (20)$$

Now the average axial strain  $\bar{\gamma} = \varepsilon_1^e/l_0$  can be used in the virtual work of the elastic forces. By this averaging, the element is no longer purely based on a displacement method, but is a hybrid element with assumed constant axial force along the element. The inclusion of non-linear terms in the expression of the first deformation mode was proposed in (Visser and Besseling, 1969), and later discussed by Crisfield (Crisfield, 1991). In (Mayo and Domínguez, 1997) a similar procedure in the context of a floating frame of reference formulation was used.

The element stiffness matrix  $\mathbf{S}^e$ , which relates the generalized stresses to the generalized strains as  $\boldsymbol{\sigma}^e = \mathbf{S}^e\varepsilon^e$ , now follows from integrating the virtual work expression for the internal forces,  $-l_0 \int_0^1 (\delta\bar{\gamma}EA\bar{\gamma} + \delta\kappa EI\kappa)d\xi = -\delta\varepsilon^{eT}\mathbf{S}^e\varepsilon^e$ , along the length of the beam as

$$\mathbf{S}^e = \begin{bmatrix} \frac{EA}{l_0} & 0 & 0 \\ 0 & s_{22}\frac{EI}{l_0^3} & -s_{24}\frac{EI}{l_0^3} \\ 0 & -s_{42}\frac{EI}{l_0^3} & s_{44}\frac{EI}{l_0^3} \end{bmatrix}, \quad (21)$$

where the numerical coefficients  $s_{ij}$  are given by the integrals

$$s_{ij} = \int_0^1 h_i''(\xi)h_j''(\xi)d\xi. \quad (22)$$

The interpolation of Eq. (9) can be related to the interpolation in the so-called absolute nodal coordinate formulation (Shabana, 1997), in which the Cartesian position coordinates and the derivatives of the position with respect to the material coordinate  $s$  at the nodes are taken as nodal coordinates. The interpolation of Eq. (9) is obtained from the absolute coordinate interpolation with the same interpolation functions  $h_i$  by the reduction of coordinates  $(\partial\mathbf{r}/\partial s)(s=0) = \mathbf{e}_x^p$ ,  $(\partial\mathbf{r}/\partial s)(s=l_0) = \mathbf{e}_x^q$ . Two coordinates are saved in the present formulation, at the expense of a mass matrix that depends on the orientation of the element. On the other hand, this connection allows a translation of the elements derived here into an absolute nodal coordinate formulation.

## Standard Beam Element

A standard beam element, as has been previously formulated (Meijaard, 1996), uses cubic interpolation polynomials,

$$\begin{aligned} h_1 &= 1 - 3\xi^2 + 2\xi^3, \\ h_2 &= \xi - 2\xi^2 + \xi^3, \\ h_3 &= 3\xi^2 - 2\xi^3, \\ h_4 &= -\xi^2 + \xi^3. \end{aligned} \quad (23)$$

These can be seen as constraint modes from a component mode synthesis perspective. The coefficients become

$$\mu_{ij} = \frac{1}{420} \begin{bmatrix} 156 & 22 & 54 & -13 \\ 22 & 4 & 13 & -3 \\ 54 & 13 & 156 & -22 \\ -13 & -3 & -22 & 4 \end{bmatrix}, \quad (24)$$

$$\beta_{22} = \frac{4}{30}, \quad \beta_{24} = \beta_{42} = -\frac{1}{30}, \quad \beta_{44} = \frac{4}{30},$$

$$s_{22} = 4, \quad s_{24} = s_{42} = 2, \quad s_{44} = 4.$$

This type of element has its use if the main function of the beam is to transfer loads between its nodes, as in a static analysis without distributed loads on the element. In a dynamic analysis, the distributed load that is needed to accelerate the mass distributed along the element is transferred to the beam by statically equivalent nodal forces. Because the element is loaded in a way that differs from the assumed load for which the interpolation is accurate, a correction to the deflection can be made in a postprocessing stage. This correction is found by calculating the additional deflection by making use of a linear kineto-elastostatic analysis. The distributed lateral acceleration along the beam is approximated by

$$(1 - \xi)\ddot{\mathbf{x}}^p \cdot \mathbf{e}_n + \xi\ddot{\mathbf{x}}^q \cdot \mathbf{e}_n + h_2(\xi)\ddot{\xi}_2^e - h_4(\xi)\ddot{\xi}_3^e. \quad (25)$$

This distribution is obtained from the interpolation (16) by neglecting non-linear terms. This gives an additional lateral deflection  $w_c \mathbf{e}_n$ , which is found from

$$\frac{2520EIw_c}{\rho Al_0^4} = -21\ddot{\mathbf{x}}^p \cdot \mathbf{e}_n (3\xi^2 - 7\xi^3 + 5\xi^4 - \xi^5) \\ - 21\ddot{\mathbf{x}}^q \cdot \mathbf{e}_n (2\xi^2 - 3\xi^3 + \xi^5) \\ - \ddot{\xi}_2^e (12\xi^2 - 22\xi^3 + 21\xi^5 - 14\xi^6 + 3\xi^7) \\ + \ddot{\xi}_3^e (-9\xi^2 + 13\xi^3 - 7\xi^6 + 3\xi^7). \quad (26)$$

Similarly, a correction for the longitudinal displacement can be made. The distributed longitudinal acceleration can be approximated by

$$(1 - \xi)\ddot{\mathbf{x}}^p \cdot \mathbf{e}_t + \xi\ddot{\mathbf{x}}^q \cdot \mathbf{e}_t, \quad (27)$$

where  $\mathbf{e}_t^T = (x^q - x^p, y^q - y^p)/l$  is a unit vector along the straight line connecting the two nodes. The additional longitudinal deflection  $u_c \mathbf{e}_t$  is found from

$$\frac{6EAu_c}{\rho Al_0^2} = -\ddot{\mathbf{x}}^p \cdot \mathbf{e}_t (-2\xi + 3\xi^2 - \xi^3) - \ddot{\mathbf{x}}^q \cdot \mathbf{e}_t (-\xi + \xi^3). \quad (28)$$

These corrections are equivalent to the corrections used in a mode acceleration method (Williams and Jones, 1948; Bisplinghoff *et al.*, 1955) and has been used in the context of flexible multibody system dynamics in (Shabana and Wehage, 1983; Ryu *et al.*, 1998). Especially for the calculation of a stress distribution this correction becomes important.

### Beam Hinged at Both Ends

In mechanisms it often happens that links are connected to other parts with hinges at which no moments are transferred or lumped rotational inertia is present. In the study of the mechanical behaviour of mechanisms, one usually starts with a kinematic analysis. After the sizes of the parts are known, a dynamic analysis based on rigid bodies is made. Stresses and deflections are calculated in an kineto-elastostatic analysis, where the forces obtained from the rigid-body analysis are used. As a last step, a full elastodynamic analysis can be made. The linear kineto-elastostatic lateral deflection  $w_{kes} \mathbf{e}_n$  of a beam that is simply supported at both ends is found from

$$\frac{360EIw_{kes}}{\rho Al_0^4} = -\ddot{\mathbf{x}}^p \cdot \mathbf{e}_n (8\xi - 20\xi^3 + 15\xi^4 - 3\xi^5) \\ - \ddot{\mathbf{x}}^q \cdot \mathbf{e}_n (7\xi - 10\xi^3 + 3\xi^5). \quad (29)$$

This analysis neglects all transient effects in the response and only gives reliable results if the mechanism is driven at a speed that is well below its main resonance frequencies.

Now no moments are applied at the hinged ends, on which the interpolation of the standard beam element is based. As there is no interaction through the rotations of the nodes with the remaining parts of the model, these rotations can be viewed as internal degrees of freedom of the element, to which some modes are assigned. In particular, these modes can be chosen in such a way that some dynamic boundary conditions are approximately satisfied. Two choices of modes will be made. In the first instance two fixed-interface linear vibration modes are used, as has been proposed by Hurty (Hurty, 1965) and Craig and Bampton (Craig and Bampton, 1968). In the second instance lateral deflection shapes that result from a linearly distributed load as occurs in a rigid body will be used, with the modes as given by the linear kineto-elastostatic analysis in Eq. (29). This corresponds to the first set of load-dependent modes as proposed by Léger (Léger, 1988). It is expected that this second choice yields better results, especially at low driving speeds, because it takes account of the way in which the beam is mainly loaded.

**Beam with Sinusoidal Modes.** If the two first sinusoidal modes corresponding to the two first eigenmodes of a simply supported beam are included, the interpolation functions be-

come

$$\begin{aligned}
h_1 &= 1 - \xi + \frac{1}{2\pi} \sin 2\pi\xi, \\
h_2 &= \frac{1}{2\pi} \sin \pi\xi + \frac{1}{4\pi} \sin 2\pi\xi, \\
h_3 &= \xi - \frac{1}{2\pi} \sin 2\pi\xi, \\
h_4 &= -\frac{1}{2\pi} \sin \pi\xi + \frac{1}{4\pi} \sin 2\pi\xi.
\end{aligned} \tag{30}$$

The coefficients become

$$\begin{aligned}
\mu_{ij} &= \frac{1}{32\pi^2} \begin{bmatrix} \frac{32}{3}\pi^2 + 20 & 22 & \frac{32}{6}\pi^2 - 20 & -10 \\ & 22 & 5 & 10 & -3 \\ \frac{32}{6}\pi^2 - 20 & 10 & \frac{32}{3}\pi^2 + 20 & -22 \\ & -10 & -3 & -22 & 5 \end{bmatrix}, \\
\beta_{22} &= \frac{1}{4}, \quad \beta_{24} = \beta_{42} = 0, \quad \beta_{44} = \frac{1}{4}, \\
s_{22} &= \frac{5}{8}\pi^2, \quad s_{24} = s_{42} = \frac{3}{8}\pi^2, \quad s_{44} = \frac{5}{8}\pi^2.
\end{aligned} \tag{31}$$

**Beam with Quintic Polynomial Interpolation.** If a quintic polynomial interpolation is used that captures the static lateral deflection as given in Eq. (29), the interpolation functions become

$$\begin{aligned}
h_1 &= 1 - 10\xi^3 + 15\xi^4 - 6\xi^5, \\
h_2 &= \xi - 6\xi^3 + 8\xi^4 - 3\xi^5, \\
h_3 &= 10\xi^3 - 15\xi^4 + 6\xi^5, \\
h_4 &= -4\xi^3 + 7\xi^4 - 3\xi^5.
\end{aligned} \tag{32}$$

The coefficients become

$$\begin{aligned}
\mu_{ij} &= \frac{1}{13860} \begin{bmatrix} 5430 & 933 & 1500 & -453 \\ & 933 & 208 & 453 & -133 \\ 1500 & 453 & 5430 & -933 \\ & -453 & -133 & -933 & 208 \end{bmatrix}, \\
\beta_{22} &= \frac{16}{70}, \quad \beta_{24} = \beta_{42} = -\frac{1}{70}, \quad \beta_{44} = \frac{16}{70}, \\
s_{22} &= \frac{192}{35}, \quad s_{24} = s_{42} = \frac{108}{35}, \quad s_{44} = \frac{192}{35}.
\end{aligned} \tag{33}$$

### Beam with a Hinged and a Built-in End

For a beam that is hinged at one node and built in at the other node, only a single internal coordinate is freely available. To describe the lateral deflection owing to a linearly varying load, another internal coordinate should be added. In order to keep the same number of nodal coordinates for each variant of the planar beam element, we are satisfied just to be able to describe the deflection caused by a constant lateral load, which is a quartic

Table 1. First two eigenfrequencies of a simply supported beam.

Type of element	No of elements	$k_1$	$k_2$
standard	1	1.1099	5.0863
standard	2	1.0039	4.4397
sinusoidal	1	1.0000	4.0000
quintic	1	1.0007	4.0325
quartic	2	1.0001	4.0023

polynomial. If it is assumed that the beam is built in at node  $p$  and hinged at node  $q$ , the quartic interpolation functions become

$$\begin{aligned}
h_1 &= 1 - 6\xi^2 + 8\xi^3 - 3\xi^4, \\
h_2 &= \xi - 3\xi^2 + 3\xi^3 - \xi^4, \\
h_3 &= 6\xi^2 - 8\xi^3 + 3\xi^4, \\
h_4 &= -3\xi^2 + 5\xi^3 - 2\xi^4.
\end{aligned} \tag{34}$$

The coefficients become

$$\begin{aligned}
\mu_{ij} &= \frac{1}{2520} \begin{bmatrix} 720 & 75 & 288 & -111 \\ & 75 & 10 & 51 & -19 \\ 288 & 51 & 1224 & -267 \\ & -111 & -19 & -267 & 76 \end{bmatrix}, \\
\beta_{22} &= \frac{3}{35}, \quad \beta_{24} = \beta_{42} = -\frac{1}{35}, \quad \beta_{44} = \frac{12}{35}, \\
s_{22} &= \frac{24}{5}, \quad s_{24} = s_{42} = \frac{18}{5}, \quad s_{44} = \frac{36}{5}.
\end{aligned} \tag{35}$$

Static corrections based on a linear analysis at a postprocessing stage as in Eqs (26) and (28) can be defined for the newly proposed beam elements. These corrections are small for the lateral deflections and are not included here; furthermore, non-linear terms can be of the same magnitude. Even for the calculation of the bending moments these corrections are small. Only the corrections for the axial displacement and force are significant.

### Comparison of Eigenfrequencies

The different variants of the planar beam element are used in the calculation of the first two linear eigenfrequencies of a simply supported beam. This beam is modelled by one standard beam, two equal standard beams, a beam with two sinusoidal modes, a beam with quintic polynomial interpolation or two beams with quartic polynomial interpolation with the built-in node in the middle. The results are shown in Table 1, which

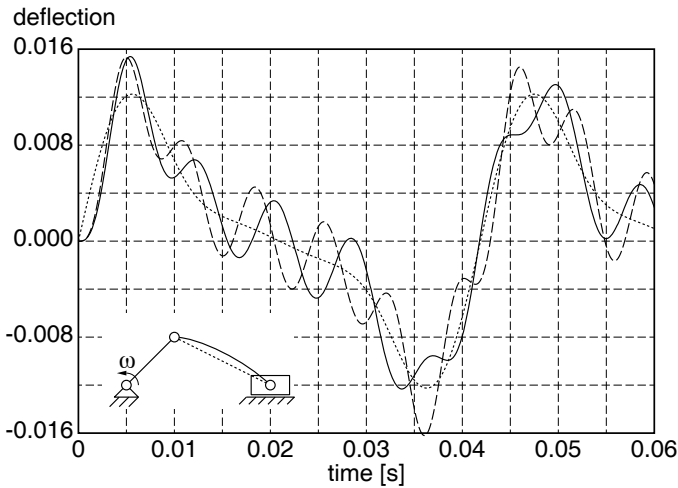


Figure 2. Non-dimensional deflection of the mid-point of a slider-crank mechanism with flexible connecting rod. Fully drawn: accurate solution with four standard elements; dashed: one standard element with correction; dotted: kineto-elastostatic deflection.

gives the factors  $k_i$  if the eigenfrequencies are expressed as

$$\omega_i = k_i \frac{\pi^2}{L^2} \sqrt{\frac{EI}{\rho A}}, \quad (36)$$

where  $L$  is the length of the beam. The beam with sinusoidal interpolation gives exact results, as expected. For a sufficiently accurate calculation of the first eigenfrequency, at least two standard beam elements are needed. A single element with a quintic polynomial interpolation yields an even better approximation, and the second eigenfrequency is obtained within one percent. Still more accurate results are obtained if two elements with a quartic polynomial interpolation are used.

## APPLICATION EXAMPLES AND COMPARISON

### Slider-Crank Mechanism

As a first example, the transient motion of a slider-crank mechanism with a rigid crank and a flexible connecting rod (Jonker, 1989; Meijaard, 1991) is considered. The crank has a length of 0.15 m, and rotates at a constant angular velocity of 150 rad/s. The connecting rod has a length of 0.30 m, a uniform mass distribution of  $\rho A = 0.2225$  kg/m and a flexural rigidity of  $EI = 12.72345$  Nm<sup>2</sup>. The slider has a mass of 0.033375 kg. In the initial position the mechanism is in its top dead centre without deformations or deformation rates. Effects of gravity or damping are excluded. As a measured quantity the lateral deflection of the

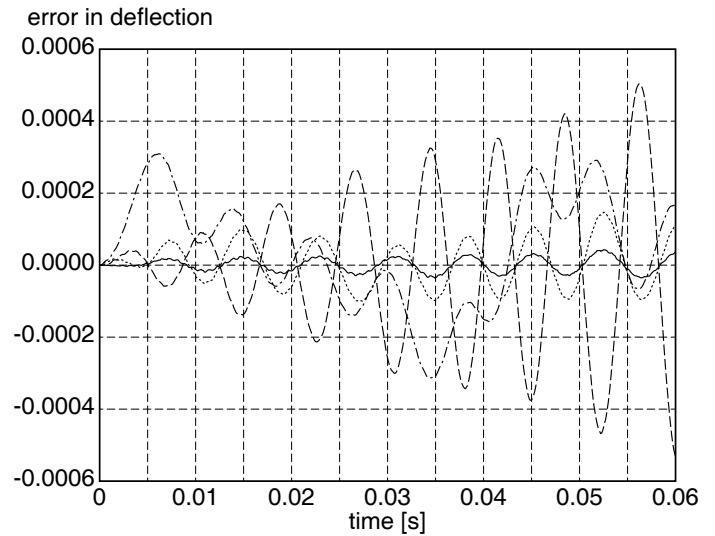


Figure 3. Error in the non-dimensional deflection of the mid-point of a slider-crank mechanism with flexible connecting rod. Dashed: two standard elements; dash-dotted: one sinusoidal element; dotted: one quintic element; fully drawn: two quartic elements.

mid-point of the connecting rod divided by its length is taken, where the deflection is defined as the distance to the straight line that connects the two end-points of the rod, the sign of which is positive if the rod deflects to the same side as it initially moves.

The crank is modelled by a rigid beam element, while the connecting rod is modelled by one or more beam elements, where the axial deformation is neglected. The cases in which the connecting rod is modelled by one, two or four standard beams, by one beam element with sinusoidal or quintic polynomial interpolation or by two beam elements with quartic polynomial interpolation are considered. The solution with four standard beam elements is taken as a reference with which other solutions are compared.

Figure 2 shows this reference solution together with the solution obtained with one standard element to which the correction according to Eq. (26) has been added, and also the kineto-elastostatic solution according to Eq. (29). The periodic kineto-elastostatic solution approximates the periodic persistent solution rather than the transient solution. Because the first eigenfrequency of the connecting rod is poorly approximated by one standard beam element, the oscillations around the kineto-elastostatic solution show a phase error that increases about linearly in time.

Figure 3 shows the errors of the other models compared with the reference solution. The solution obtained with two standard beam element is the poorest and shows an error amplitude that grows linearly in time, which means that the error in the approx-

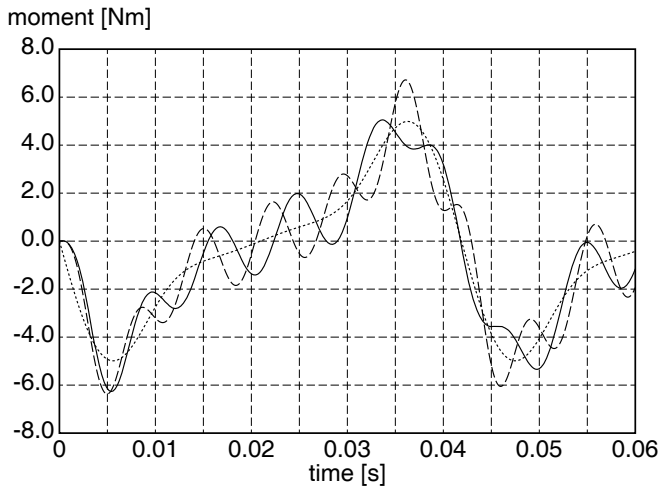


Figure 4. Bending moment at the mid-point of a slider-crank mechanism with flexible connecting rod. Fully drawn: accurate solution with four standard elements with correction; dashed: one standard element with correction; dotted: kineto-elastostatic solution.

imation of the first eigenfrequency contributes strongly to the error in deflection. The accuracies obtained with one beam element with quintic polynomial or sinusoidal interpolation are comparable, although the quintic element gives a better accuracy. The solution obtained with two beam elements with quartic polynomial interpolation is still more accurate, but the model has two additional degrees of freedom.

As a second measured quantity, the bending moment at the mid-point of the connecting rod is considered, which is close to the point where the maximal bending moments are found. A moment that bends the beam into a convex shape has a positive sign. If there is a node at this mid-point, the average bending moment in the two adjacent elements at their respective ends is used. Figure 4 shows the solution obtained with four standard beam elements as a reference, together with the kineto-elastostatic solution and the solution obtained with one standard beam element. The relative errors in these last two solutions comparable to those in the deflection. Figure 5 shows the errors, compared to the reference solution, for the other models. Also for these models, the relative errors in the bending moments are of the same order of magnitude as those in the deflections; only the error in the results obtained with two quartic elements is larger and is comparable to the error obtained with one quintic element.

We can conclude that, for this example, modelling the beam with one quintic element gives results that are sufficiently accurate for most applications. Although the element with sinusoidal interpolation gives a better approximation for the eigenfrequencies, the quintic element still gives better results, apparently because it takes into account how the element is loaded.

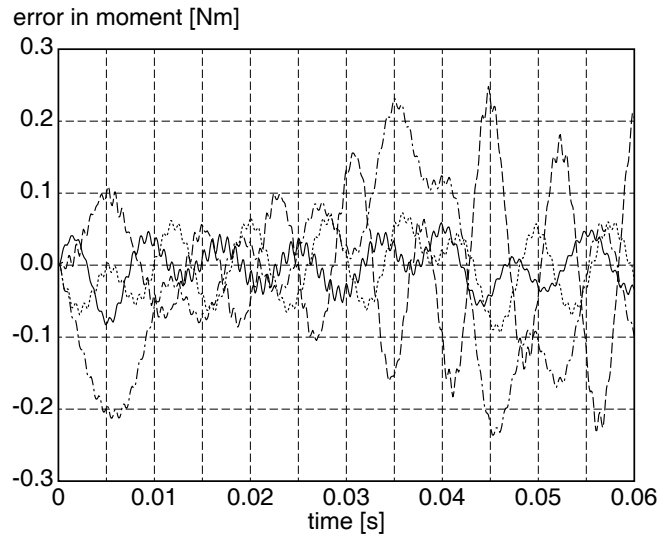


Figure 5. Error in the bending moment at the mid-point of a slider-crank mechanism with flexible connecting rod. Dashed: two standard elements; dash-dotted: one sinusoidal element; dotted: one quintic element; fully drawn: two quartic elements.

### Spin-Up Motion of a Cantilevered Beam

The second example deals with the spin-up motion of a beam whose base is attached to a rigid shaft with an axis that is perpendicular to that of the beam. The parameters for the system are the same as those given in (Kim and Haug 1988; Wu and Haug 1988) and which were used previously in (Meijaard, 1996). The shaft is given a prescribed angular displacement  $\psi$  that accelerates the beam from a state of rest to a rotation with an angular velocity  $\dot{\psi} = \omega = 4 \text{ rad/s}$  in the time interval of length  $T = 15 \text{ s}$ , after which the angular velocity remains constant. If the motion starts at  $t = 0$ , the rotation angle is given by

$$\psi = \frac{\omega}{T} \left[ \frac{t^2}{2} + \frac{T^2}{4\pi^2} \left( \cos \frac{2\pi t}{T} - 1 \right) \right] \quad (0 \leq t \leq T),$$

$$\psi = \omega \left( t - \frac{1}{2}T \right) \quad (t > T).$$
(37)

The length of the beam is 8 m, it has a rectangular cross-section with height of 36.75 mm and width of 1.986 mm, the material has a density  $\rho = 2766.67 \text{ kg/m}^3$  and Young's modulus  $E = 68.95 \text{ GPa}$ . The measured quantity is the lateral deflection of the tip of the beam, which is the distance of the tip to the line that is tangent to the beam at the base, where a lead gives a positive deflection.

The beam is modelled with one or two standard beam elements or by a single beam element with quartic polynomial interpolation. The axial deformation of the beam is neglected. The

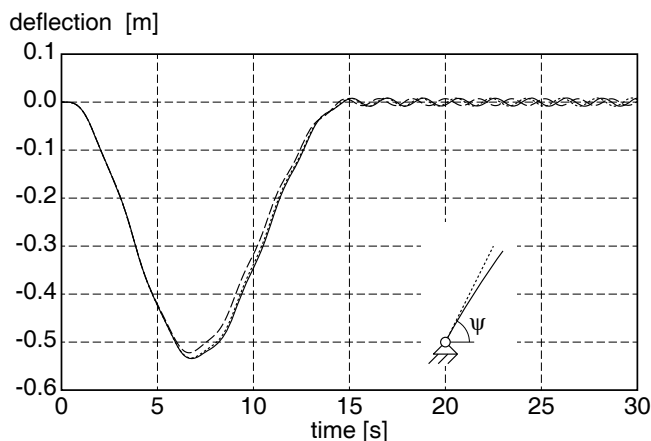


Figure 6. Lateral deflection of a cantilevered beam in a spin-up motion. Fully drawn: accurate solution with two standard elements; dashed: one standard element; dotted: one quartic element.

solution obtained with two standard elements is taken as a reference solution. Figure 6 shows the results for the three cases. Whereas the solution obtained with a single standard beam element has an error in the maximal deflection of about 6%, the solution with a single quartic element gives a solution that has an error of about 1.5%, which is a reasonably good approximation. The first eigenfrequency of the spinning beam is better approximated than in the model with the standard beam element.

Of course, an element could have been developed specially for this problem with a quintic interpolation polynomial which satisfies the conditions of a zero shear force and moment at the end and takes account of the special distribution of the normal force along the beam. We preferred to show the performance of an element which has a wider range of applicability.

## CONCLUSIONS

A family of planar beam elements has been developed, which can make use of the fact that one or both ends are hinged. It has been shown that the effects of geometric non-linearities can be properly included. Load-dependent modes rather than normal vibration modes appear to be the natural choice for components that can make large gross motions. In the example of the slider-crank mechanism with a flexible connecting rod, the load-dependent modes resulted in more accurate solutions.

By the way in which the planar beam elements were developed, a generalization seems possible. The extension to spatial beams and non-uniform beams is straightforward, while the possibility of deriving superelements for quite general substructures is a subject of further investigation.

## REFERENCES

- Bisplinghoff, R.L., Ashley, H., and Halfman, R.L., 1955, *Aeroelasticity*, Addison-Wesley, Cambridge MA.
- Craig, R.R., Jr, 1981, *Structural Dynamics: An Introduction to Computer Methods*, John Wiley and Sons, New York.
- Craig, R.R., Jr, 1995, "Substructure Methods in Vibration," *ASME Journal of Mechanical Design*, **117**, pp. 207–213.
- Craig, R.R., Jr, and Bampton, M.C.C., 1968, "Coupling of Substructures for Dynamic Analyses," *AIAA Journal*, **6**, pp. 1313–1319.
- Crisfield, M.A., 1991, *Non-Linear Finite Element Analysis of Solids and Structures, Volume 1: Essentials*, John Wiley and Sons, Chichester.
- Greif, R., 1986, "Substructuring and Component Mode Synthesis," *The Shock and Vibration Digest*, **18**(7), pp. 3–8.
- Guyan, R.J., 1965, "Reduction of Stiffness and Mass Matrices," *AIAA Journal*, **3**, p. 380.
- Hunn, B.A., 1953, "A Method of Calculating Space Free Resonance Modes of an Aircraft," *The Journal of the Royal Aeronautical Society*, **57**, pp. 420–422.
- Hunn, B.A., 1955, "A Method of Calculating the Normal Modes of an Aircraft," *The Quarterly Journal of Mechanics and Applied Mathematics*, **8**, pp. 38–58.
- Hurty, W.C., 1960, "Vibrations of Structural Systems by Component Mode Synthesis," *ASCE Journal of the Engineering Mechanics Division*, **86**(EM4), pp. 51–69.
- Hurty, W.C., 1965, "Dynamic Analysis of Structural Systems Using Component Modes," *AIAA Journal*, **3**, pp. 678–685.
- Irons, B., 1965, "Structural Eigenvalue Problems: Elimination of Unwanted Variables," *AIAA Journal*, **3**, pp. 961–962.
- Jonker, J.B., 1989, "A Finite Element Dynamic Analysis of Spatial Mechanisms with Flexible Links," *Computer Methods in Applied Mechanics and Engineering*, **76**, pp. 17–40.
- Jonker, J.B., and Meijaard, J.P., 1990, "SPACAR—Computer Program for Dynamic Analysis of Flexible Spatial Mechanisms and Manipulators," in Schiehlen, W., *Multibody Systems Handbook*, Springer, Berlin, pp. 123–143.
- Kim, S.-S., and Haug, E.J., 1988, "A Recursive Formulation for Flexible Multibody Dynamics, Part I: Open-Loop Systems," *Computer Methods in Applied Mechanics and Engineering*, **71**, pp. 293–314.
- Léger, P., 1988, "Load Dependent Subspace Reduction Methods for Structural Dynamic Computations," *Computers and Structures*, **29**, pp. 993–999.
- Mayo, J., and Domínguez, J., 1997, "A Finite Element Geometrically Nonlinear Dynamic Formulation of Flexible Multibody Systems Using a New Displacements Representation," *ASME Journal of Vibration and Acoustics*, **119**, pp. 573–581.
- Meijaard, J.P., 1991, "Direct Determination of Periodic Solutions of the Dynamical Equations of Flexible Mechanisms and Manipulators," *International Journal for Numerical Methods in Engineering*, **32**, pp. 1691–1710.

Meijaard, J.P., 1996, "Validation of Flexible Beam Elements in Dynamics Programs," *Nonlinear Dynamics*, **9**, pp. 21–36.

Noor, A.K., 1994, "Recent Advances and Applications of Reduction Methods," *Applied Mechanics Reviews*, **47**, pp. 125–146.

Ryu, J., Kim, H.-S., and Wang, S., 1998, "A Method for Improving Dynamic Solutions in Flexible Multibody Dynamics," *Computers and Structures*, **66**, pp. 765–776.

Seshu, P., 1996, "Review: Substructuring and Component Mode Synthesis," *Shock and Vibration*, **4**, pp. 199–210.

Shabana, A.A., 1997, "Flexible Multibody Dynamics: Review of Past and Recent Developments," *Multibody System Dynamics*, **1**, pp. 189–222.

Shabana, A., and Wehage, R.A., 1983, "Variable Degree-of-Freedom Component Mode Analysis of Inertia Variant Flexible Mechanical Systems," *ASME Journal of Mechanisms, Transmissions, and Automation in Design*, **105**, pp. 371–378.

Visser, W., and Besseling, J.F., 1969, "Large Displacement Analysis of Beams," Report WTHD 10, Department of Mechanical Engineering, Delft University of Technology, Delft.

Williams, D., and Jones, R.P.N., 1948, "Dynamic Loads in Aeroplanes under Given Impulsive Loads with Particular Reference to Landing and Gust Loads on a Large Flying Boat," *Aeronautical Research Council Reports and Memoranda No 2221*, His Majesty's Stationery Office, London.

Wilson, E.L., Yuan, M.-W., and Dickens, J.M., 1982, "Dynamic Analysis by Direct Superposition of Ritz Vectors," *Earthquake Engineering and Structural Dynamics*, **10**, pp. 813–821.

Wu, S.-C., and Haug, E.J., 1988, "Geometric Non-Linear Substructuring for Dynamics of Flexible Mechanical Systems," *International Journal for Numerical Methods in Engineering*, **26**, pp. 2211–2226.

Yeh, H.-F., and Dopker, B., 1990, "Deformation Mode Selection and Mode Orthonormalization for Flexible Body System Dynamics," *Computers and Structures*, **34**, pp. 615–627.